

RESEARCH ARTICLE

In silico identification and experimental validation of hits active against KPC-2 β -lactamase

Raphael Klein¹, Pasquale Linciano², Giuseppe Celenza³, Pierangelo Bellio³, Sofia Papaioannou², Jesus Blazquez⁴, Laura Cendron⁵, Ruth Brenk^{6*}, Donatella Tondi^{2*}

1 Institute of Pharmacy and Biochemistry, Johannes Gutenberg University, Mainz, Germany, **2** Dipartimento di Scienze della Vita, Università di Modena e Reggio Emilia, Modena, Italy, **3** Dipartimento di Scienze Cliniche Applicate e Biotecnologie, Università dell'Aquila, L'Aquila, Italy, **4** Department of Microbial Biotechnology, National Center for Biotechnology, Consejo Superior de Investigaciones Científicas (CSIC), Campus de la Universidad Autónoma-Cantoblanco, Madrid, Spain, **5** Dipartimento di Biologia, Università di Padova, Padova, Italy, **6** Department of Biomedicine, University of Bergen, Bergen, Norway

☞ These authors contributed equally to this work.

* donatella.tondi@unimore.it (DT); Ruth.Brenk@uib.no (RB)



OPEN ACCESS

Citation: Klein R, Linciano P, Celenza G, Bellio P, Papaioannou S, Blazquez J, et al. (2018) *In silico* identification and experimental validation of hits active against KPC-2 β -lactamase. PLoS ONE 13 (11): e0203241. <https://doi.org/10.1371/journal.pone.0203241>

Editor: Alessio Lodola, University of Parma, ITALY

Received: August 15, 2018

Accepted: November 6, 2018

Published: November 29, 2018

Copyright: © 2018 Klein et al. This is an open access article distributed under the terms of the [Creative Commons Attribution License](https://creativecommons.org/licenses/by/4.0/), which permits unrestricted use, distribution, and reproduction in any medium, provided the original author and source are credited.

Data Availability Statement: All relevant data are within the paper.

Funding: Funded by Fondo di Ricerca di Ateneo UNIMORE (DT). The funders had no role in study design, data collection and analysis, decision to publish, or preparation of the manuscript.

Competing interests: The authors have declared that no competing interests exist.

Abstract

Bacterial resistance has become a worldwide concern, particularly after the emergence of resistant strains overproducing carbapenemases. Among these, the KPC-2 carbapenemase represents a significant clinical challenge, being characterized by a broad substrate spectrum that includes aminothiazoleoxime and cephalosporins such as cefotaxime. Moreover, strains harboring KPC-type β -lactamases are often reported as resistant to available β -lactamase inhibitors (clavulanic acid, tazobactam and sulbactam). Therefore, the identification of novel non β -lactam KPC-2 inhibitors is strongly necessary to maintain treatment options. This study explored novel, non-covalent inhibitors active against KPC-2, as putative hit candidates. We performed a structure-based *in silico* screening of commercially available compounds for non- β -lactam KPC-2 inhibitors. Thirty-two commercially available high-scoring, fragment-like hits were selected for *in vitro* validation and their activity and mechanism of action vs the target was experimentally evaluated using recombinant KPC-2. N-(3-(1H-tetrazol-5-yl)phenyl)-3-fluorobenzamide (**11a**), in light of its ligand efficiency (LE = 0.28 kcal/mol/non-hydrogen atom) and chemistry, was selected as hit to be directed to chemical optimization to improve potency vs the enzyme and explore structural requirement for inhibition in KPC-2 binding site. Further, the compounds were evaluated against clinical strains overexpressing KPC-2 and the most promising compound reduced the MIC of the β -lactam antibiotic meropenem by four-fold.

Introduction

The emergence of KPC-2 class-A β -Lactamase (BL) carbapenemase, which confers resistance to last resort carbapenems, poses a serious health threat to the public. KPC-2, a class A BL,

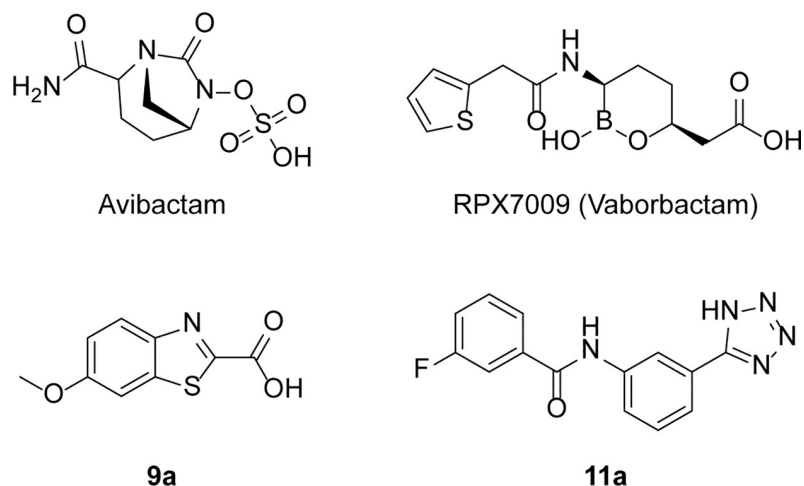


Fig 1. Chemical structure of avibactam, RPX7009, and compounds 9a and 11a.

<https://doi.org/10.1371/journal.pone.0203241.g001>

uses a catalytic serine to hydrolyze the β -lactam ring. Specifically, the hydrolysis reaction proceeds through a series of steps involving: (i) the formation of a pre-covalent complex, (ii) the conversion to a high-energy tetrahedral acylation intermediate, (iii) followed by a low-energy acyl-enzyme complex, (iv) a high-energy tetrahedral de-acylation intermediate consequent to catalytic water attack, and (v) finally the release of the hydrolyzed β -lactam ring product from the enzyme. [1–6].

Notably to treat infections caused by bacteria that produce class A BLs, mechanism-based inhibitors (i.e., clavulanic acid, sulbactam, and tazobactam) are administered in combination with β -lactam antibiotics. However, strains harboring KPC-type β -lactamases are reported to be resistant to available β -lactamase inhibitors. Moreover, because of KPC-2's broad spectrum of activity (which includes penicillins, cephalosporins, and carbapenems) treatment options against KPC-2-producing bacteria are scarce, and "last-resort" carbapenems are ineffective as well [7]. Therefore, studies directed to the discovery of novel, non β -lactam KPC-2 inhibitors have multiplied in the last years. Recently, new drugs able to restore susceptibility to β -lactams i.e. the novel inhibitor avibactam in combination with ceftazidime (CAZ) and RPX7009 (vaborbactam) with meropenem have been approved (Fig 1)[8–10].

As attention on KPC-2 rises, the number of crystal structures of its apo and complexed form disclosed in the PDB has increased, making KPC-2 a druggable target for structure based drug design efforts and for the study of novel, non β -lactam like inhibitors of this threatening carbapenemase [9–12]

Recently, two crystal structures of the hydrolyzed β -lactam antibiotics cefotaxime and faropenem in complex with KPC-2 were determined (PDB codes 5UJ3, 5UJ4; Fig 2).[13]

Both ligands form hydrogen-bond interactions with their C4-carboxyl group to Ser130, Thr235 and Thr237. The dihydrothiazine moiety of cefotaxime and the dihydrothiazole moiety of faropenem forms π - π -stacking interactions with Trp105. In the apo-enzyme, this side chain adopts two rotamers, upon binding of a ligand just one. Mutagenesis studies have shown the importance of Trp105 in substrate recognition [7]. The faropenem ring nitrogen forms a hydrogen-bond interaction with Ser130, whereas the ring nitrogen of cefotaxime a hydrogen bond with Ser70. The aminothiazole ring of cefotaxime forms van-der-Waals contacts with Leu167, Asn170, Cys238 and Gly239, while the oxyimino group and the hydroxyethyl group of faropenem are solvent exposed (Fig 2).[13]

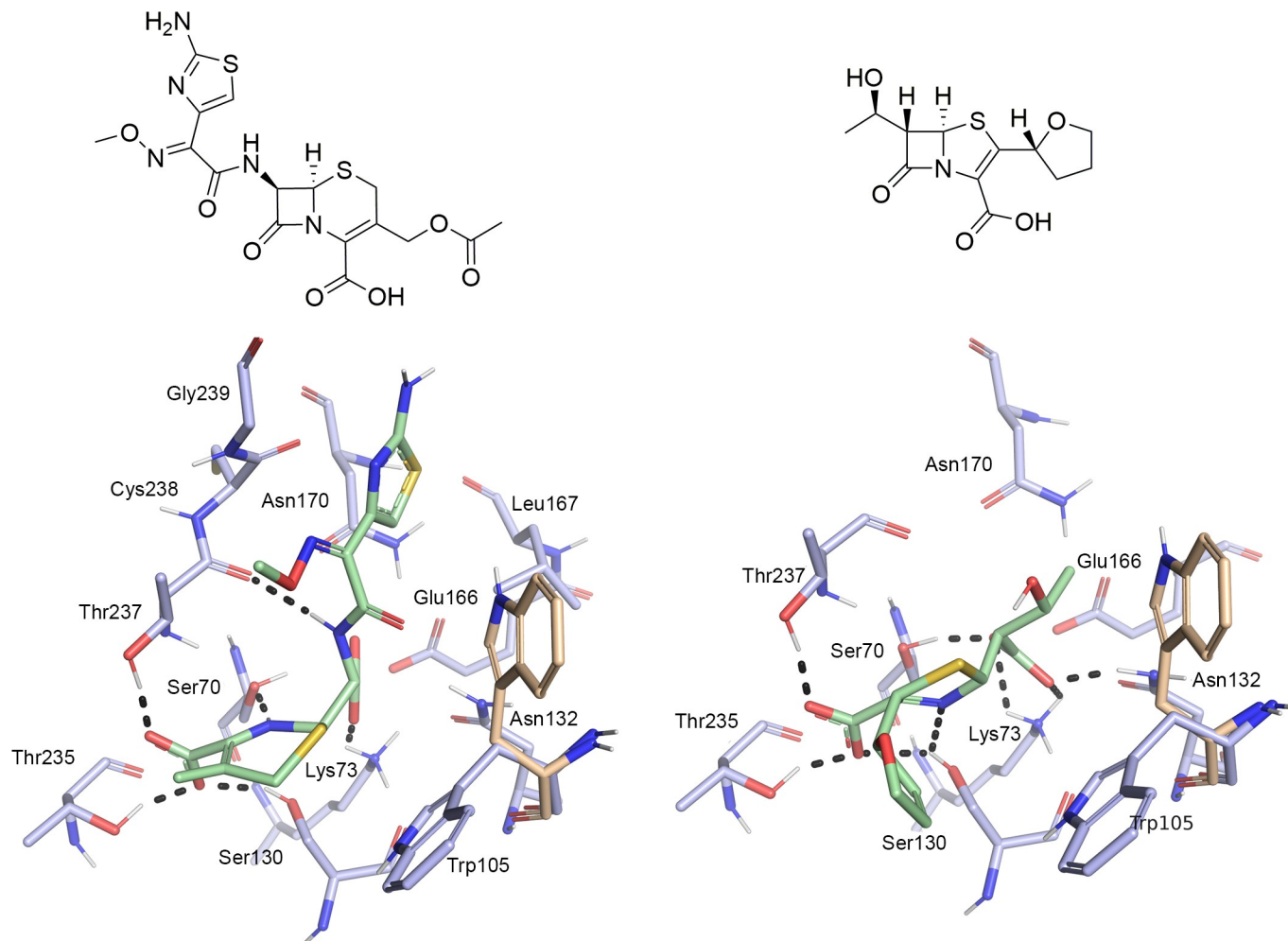


Fig 2. Structures and binding modes of hydrolyzed β -lactam antibiotics in the KPC-2 binding site. Left: binding mode of hydrolyzed cefotaxime (PDB code 5UJ3). Right: binding mode of hydrolyzed faropenem (PDB code 5UJ4). The second rotamer of Trp105 adopted in the apo-enzyme is coloured in beige, protein side chains in blue and ligands in green. Hydrogen bonds are indicated as black dots.

<https://doi.org/10.1371/journal.pone.0203241.g002>

Based on this and other structural information, we used a hierarchical screening cascade for the discovery of non β -lactam like KPC-2 inhibitors. The selected 32 candidates, most of them fragment-like, were then validated as hits against isolated recombinant KPC-2. Among the tested compounds **9a**, a benzothiazole derivative, and **11a**, a tetrazole-containing inhibitor, showed the highest activity against KPC-2 and behaved as competitive inhibitors of the targeted carbapenemase (Fig 1). Subsequently, compound **11a**, in light of its promising ligand efficiency and chemistry, was selected to undergo chemical optimization for potency improvement and to explore structural requirement for inhibition in KPC-2 binding site. Further, the obtained compounds were evaluated against clinical strains overexpressing KPC-2 and the most promising compound reduced the MIC of the β -lactam antibiotic meropenem by four fold.

Materials and methods

Pharmacophore hypothesis

A search for similar binding sites of KPC-2 was carried out using the online tool PoSSuM—Search K [14,15]. Based on shared ligand interactions in the retrieved structures (Table 1), a

Table 1. Result of PoSSuM Search K for similar binding sites. Structures with binding sites similar with structure 3RXW in complex with a non-covalent ligand were reported.

	PDB-code	Protein name	Resolution	Ref.
1	4BD0	<i>E. coli</i> β -lactamase TOHO-1	1.21 Å	[18]
2	3G30	<i>E. coli</i> β -lactamase CTX-M-9a	1.80 Å	[19]
3	4DE1	<i>E. coli</i> β -lactamase CTX-M-9a	1.26 Å	[17]
4	4DDY	<i>E. coli</i> β -lactamase CTX-M-9a	1.36 Å	[17]
5	4DE3	<i>E. coli</i> β -lactamase CTX-M-9a	1.44 Å	[17]
6	4DDS	<i>E. coli</i> β -lactamase CTX-M-9a	1.36 Å	[17]
7	4DE0	<i>E. coli</i> β -lactamase CTX-M-9a	1.12 Å	[17]
8	4EUZ	<i>S. fonticola</i> β -lactamase SFC-1	1.08 Å	[20]
9	4DE2	<i>E. coli</i> β -lactamase CTX-M-9a	1.40 Å	[17]
10	3G35	<i>E. coli</i> β -lactamase CTX-M-9a	1.41 Å	[19]
11	3G32	<i>E. coli</i> β -lactamase CTX-M-9a	1.31 Å	[19]
12	3G2Y	<i>E. coli</i> β -lactamase CTX-M-9a	1.31 Å	[19]
13	3G31	<i>E. coli</i> β -lactamase CTX-M-9a	1.70 Å	[19]

<https://doi.org/10.1371/journal.pone.0203241.t001>

pharmacophore was defined based on a *K. pneumoniae* KPC-2 protein structure (PDB code 3RXW) [16] and the ligand OJ6 of CTX-M-9 β -lactamase (PDB code 4DE1) [17]. The derived pharmacophore contained a hydrogen-bond acceptor feature for interaction with Thr237, Thr235 and Ser130, a hydrophobic feature for π -stacking with Trp105 and a hydrogen bond acceptor feature for interactions with Asn132 (Fig 3).

Virtual screening

Our in-house MySQL-database of commercially available compounds was used as basis for virtual screening. This database contains catalogues from the following suppliers: Apollo

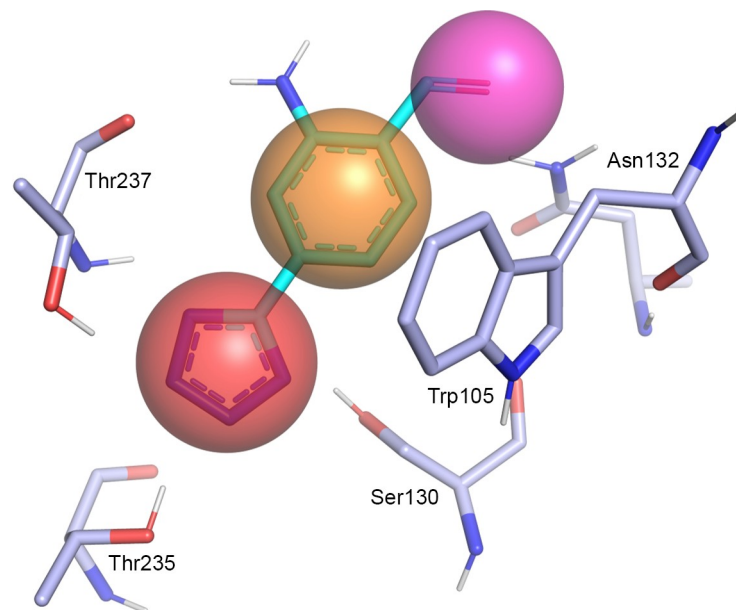


Fig 3. Pharmacophore hypothesis for KPC-2 ligands. Binding site of KPC-2 (PDB code 3RXW, blue) superimposed with a fragment of the ligand OJ6 bound to CTX-M-9 β -lactamase (PDB code 4DE1, cyan) and pharmacophore features (red: hydrogen-bond acceptor, orange: hydrophobic interaction feature, purple: hydrogen-bond donor) (Ambler numbering) [21].

<https://doi.org/10.1371/journal.pone.0203241.g003>

Scientific, Asinex, Chembridge, Chemdiv, Enamine, InterBioScreen, Key Organics, Life Chemicals, Maybridge, MicroCombiChem, Otava, Peakdale, Sigma-Aldrich, Specs, Timtec, Vitas-M laboratory, and Zylexa Pharma. The compounds were standardized and filtered for compounds fulfilling the following lead-like criteria: between 10 and 25 heavy atoms, between one and six hydrogen-bond acceptors, between one and three hydrogen-bond donors and a clog P between -3 and 3. In addition, the complexity was limited by only including compounds with less than 7 rotatable bonds and between 1 and 3 ring systems. Compounds containing unwanted reactive or toxic functional groups were excluded as well [22].

In-house python scripts based on OpenEye's OEChem toolkit (OEChem, version 2016.6.1, OpenEye Scientific Software, Inc., Santa Fe, NM, USA) were used to charge, tautomerize and stereoisomerize the selected compounds (scripts are available at https://github.com/ruthbrenk/compound_preparation). Conformers were generated using OpenEye's OMEGA toolkit [23]. The pharmacophore filtering was carried out using Molecular Operating Environment (MOE, Chemical Computing Group). Compounds that passed the pharmacophore filter were transformed into a format suitable for docking as described previously [24].

The crystal structure of *K. pneumoniae* KPC-2 (PDB code 3RXW) [16] was used as receptor for docking. The 'protonate 3D' tool of MOE was used to add polar hydrogen atoms to the receptor, energy minimize their positions and to assign partial charges based on the AMBER force field parameters. Water molecules and ligands (CIT and SR3) were deleted and the position of the Ser69 side chain was energy minimized with the same force field parameters. The structure was aligned with the crystal structure of *E.coli* CTX-M-9 (PDB code 4DE1) and the ligand 0J6 was used to define spheres as matching points for docking. Grid-based excluded volume, van-der-Waals potential and electrostatic potential as well as solvent occlusion maps were calculated as described earlier [25,26].

The compounds were docked into the binding site of KPC-2 using DOCK3.6 [26–28]. Parameters for sampling ligand orientations were set as follows: bin size of ligand and receptor were set to 0.4 Å, overlap bins were set to 0.2 Å and the distance tolerance for receptor and ligand matching spheres was set to 1.5 Å. Each docking pose which did not overlap with the receptor was scored for electrostatic and van-der-Waals complementarity and penalized according to its estimated partial desolvation energy. For each compound, only the best-scoring pose out of its tautomers, protonation states or ring alignments was saved in the final docking hit list. The docking hit list was filtered with the pharmacophore described above, keeping the ligand positions rigid. Compounds passing this filter were ranked by their calculated ligand efficiency [29,30] and inspected by eye.

Expression and purification of recombinant KPC-2

The *bla*_{KPC-2} gene was kindly provided by Prof. Sergei Vakulenko (University of Notre Dame du Lac, Indiana, USA) and cloned as already reported [31] and transformed into competent *E. coli* BL21 (DE3) cells for protein expression. 50 mL of Tryptic Soy Broth (TSB) (50 mg/L kanamycin) were inoculated with fresh colonies and grown at 37°C. 4 mL of the overnight culture was used to inoculate 1.3 L of TSB (50 mg/L kanamycin) grown at 37°C with shaking to an optical density of 0.5 measured at 600 nm. Then expression of recombinant *bla* gene was induced by adding 1.0 mM IPTG (isopropyl-D-thiogalactopyranoside) and the cells were again allowed to grow at 20°C overnight. Bacteria were harvested by centrifugation at 4000 rpm for 20 minutes. The pelleted cells were resuspended in Tris-HCl 50 mM pH 7.4–7.5. Periplasmic proteins were extracted as reported in the pET System Manual (TB055 10th Edition Rev. B 0403) and subsequently dialyzed in sodium acetate buffer (50 mM, pH 5.0). The protein was conveniently purified in a single step using a Macro-Prep High S resin and eluted using

sodium acetate 50 mM pH 5.0 and a sodium chloride (NaCl) linear gradient from 100 to 500 mM. The purified protein was dialyzed overnight in sodium phosphate buffer 50 mM, pH 7.0 [31,32].

Inhibition assays

The hydrolytic activity of KPC-2 was measured using the β -lactam substrates CENTA (100 μ M, K_M 70 μ M) or nitrocefin (114 μ M, K_M 36 μ M) in reaction buffer consisting of 50 mM of PB at pH 7.0 at 25°C with 0.01% v/v Triton X-100 to avoid compound aggregation and promiscuous inhibition.[33] Reactions were monitored using a Beckmann DU640 spectrophotometer at 405nm for CENTA and 480 nm wavelength for nitrocefin [34]. The test compounds were synthesized as described below or purchased from Enamine, TimTec, Vitas-M, ChemBridge, Otava, Life Chemicals or Apollo Scientific and assayed without further purification. Compounds were dissolved in dimethyl sulfoxide (DMSO) to a concentration of 25 mM and stored at -20°C. The highest concentration at which the compounds were tested was up to 1 mM (depending on their solubility). All experiments were performed in duplicate and the error never exceeded 5%. The reaction was typically initiated by adding KPC-2 to the reaction buffer last. To control for incubation effects, protein was added to the reaction buffer first, and the reaction was initiated by the addition of reporter substrate after 10 minutes of enzyme-compound incubation. The results are reported in Fig 4 and Fig 5.

Competitive inhibition mechanism and the K_i for compound **9a** was determined by Lineweaver–Burk (LB) and Dixon plots. For compound **11a**, already reported as competitive inhibitor of the extended spectrum β -lactamase (ESBL) CTX-M15, the K_i was calculated by the Cheng-Prusoff equation ($K_i = IC_{50}/(1 + [S]/K_M)$) assuming competitive inhibition [35].

Synthetic procedures

All commercially available chemicals and solvents were reagent grade and were used without further purification unless otherwise specified. Reactions were monitored by thin-layer chromatography on silica gel plates (60F-254, E. Merck) and visualized with UV light, cerium ammonium sulfate or alkaline $KMnO_4$ aqueous solution. The following solvents and reagents have been abbreviated: ethyl ether (Et_2O), dimethyl sulfoxide (DMSO), ethyl acetate ($EtOAc$), dichloromethane (DCM), methanol (MeOH). All reactions were carried out with standard techniques. NMR spectra were recorded on a Bruker 400 spectrometer with 1H at 400.134 MHz and ^{13}C at 100.62 MHz. Proton chemical shifts were referenced to the TMS internal standard. Chemical shifts are reported in parts per million (ppm, δ units). Coupling constants are reported in units of Hertz (Hz). Splitting patterns are designed as s, singlet; d, doublet; t, triplet; q quartet; dd, double doublet; m, multiplet; b, broad. Mass spectra were obtained on a 6310A Ion TrapLC-MS(n).

General procedure for the synthesis of sulfonamides 1-6b. To a solution of 3-(1H-tetrazol-5-yl)aniline (1 eq.) in DCM dry (25 mL) at room temperature and under nitrogen atmosphere, pyridine (3 eq.) and the appropriate sulfonyl-chloride (1.2 eq.) were added. The mixture was reacted at room temperature for 2–12 h. The reaction was quenched with aqueous saturated solution of NH_4Cl and acidified at pH 4 with aqueous 1N HCl. The aqueous phase was extracted with AcOEt, and the organic phase washed with brine, dried over Na_2SO_4 and concentrated. The crude was crystalized from MeOH or Et_2O to give the desired product.

N-(3-(1H-tetrazol-5-yl)phenyl)-3-fluorobenzenesulfonamide (1b). Pale yellow solid (150 mg, yield 47%). 1H NMR (400 MHz, DMSO- d_6) δ 7.19 (dd, $J = 2.2, 8.1$ Hz, 1H), 7.33–7.45 (m, 2H), 7.47–7.58 (m, 3H), 7.62 (d, $J = 7.7$ Hz, 1H), 7.76 (t, $J = 1.8$ Hz, 1H), 10.61 (s, 1H), the H of tetrazole exchanges. MS m/z $[M+H]^+$ 320.1; $[M-1]^-$ 318.0.

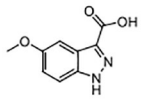
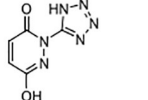
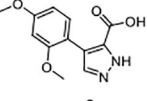
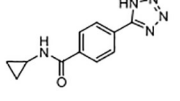
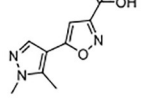
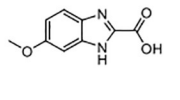
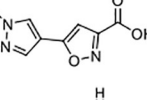
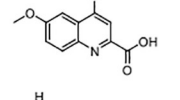
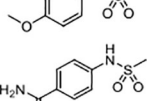
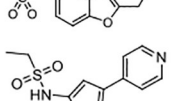
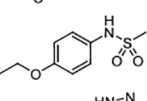
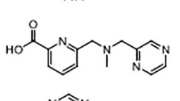
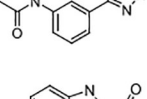
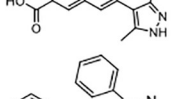
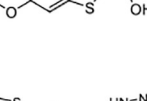
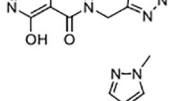
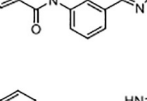
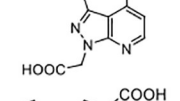
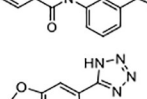
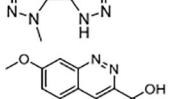
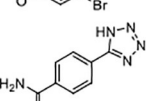
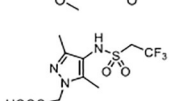
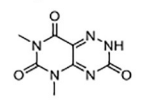
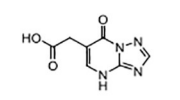
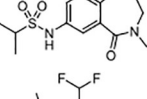
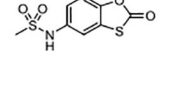
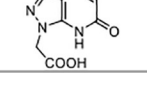
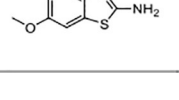
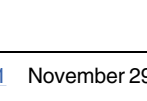
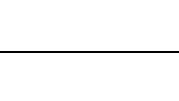


ID	Structure	IC ₅₀ mM ^[a,b]	ID	Structure	IC ₅₀ mM ^[a,b]
1a		> 0.33 (30)	17a		>1.0 (23)
2a		> 0.50 (38)	18a		1.0 (18)
3a		>0.25 (13)	19a		0.88
4a		>0.25 (12)	20a		>0.5 (28) ^[c]
5a		>0.50 (13)	21a		>1.0 (12)
6a		>1.0 (18)	22a		NI at 1.0
7a		>1.0 (12)	23a		>1.0 (26) ^[c]
8a		>0.50 (37)	24a		>0.1 (41)
9a		0.15 ^[c]	25a		> 0.4 (26)
10a		0.07 ^[c]	26a		> 0.83 (18)
11a		0.036 ^[c]	27a		NI at 0.5
12a		0.70 ^[c]	28a		>0.5 (14)
13a		NI at 0.25	29a		>1.0 (15)
14a		>1.0 (26)	30a		NI at 1.0
15a		>0.66 (38)	31a		>1.0 (11)
16a		>1.0 (17)	32a		1.24

Fig 4. Inhibitory activity of compounds selected from virtual screening. ^[a] Assays were performed in duplicate (errors were less than 5%) with CENTA as reporter substrate (100 μ M, k_m 70 μ M). Kinetic were monitored at 25° by following the absorbance variation at $\lambda = 405$ nm. ^[b] If no IC_{50} has been measured, percent inhibition at the highest tested concentration is given in parentheses. For example, > 0.50 (26%) implies that the highest concentration tested was 0.50 mM; at this concentration, the enzyme was inhibited by 26%. Therefore, $IC_{50} > 0.50$ mM. When % Inhibition was below 10% No Inhibition (NI) is reported. ^[c] Assays were run after 10' incubation of the inhibitor with KPC-2. Reaction was started by the addition of CENTA.

<https://doi.org/10.1371/journal.pone.0203241.g004>

N-(3-(1H-tetrazol-5-yl)phenyl)-3-nitrobenzenesulfonamide (2b). Pink solid (62% yield). ¹H-NMR (400 MHz, DMSO-d₆) δ : 7.31 (ddd, $J = 1.0, 2.3, 8.2$ Hz, 1H), 7.51 (t, $J = 8.0$ Hz, 1H), 7.74 (dt, $J = 1.2, 7.8$ Hz, 1H), 7.82–7.96 (m, 2H), 8.18 (dt, $J = 1.3, 7.9$ Hz, 1H), 8.46 (ddd, $J = 1.0, 2.3, 8.2$ Hz, 1H), 8.54 (t, $J = 2.0$ Hz, 1H), 10.90 (s, 1H); the H of tetrazole exchanges. ¹³C-NMR (DMSO-d₆) δ : 117.35, 120.09, 123.04, 127.35, 129.17, 129.22, 129.69, 133.21, 136.59, 137.99, 139.81, 148.82, 154.28. MS m/z [M+H]⁺ Calcd for C₁₃H₁₀N₆O₄S: 346.0 Found: 347.2.

N-(3-(1H-tetrazol-5-yl)phenyl)-5-(dimethylamino)naphthalene-1-sulfonamide (3b). White solid (31% yield). ¹H NMR (400 MHz, DMSO-d₆) δ 2.78 (s, 6H), 7.20 (dd, $J = 1.5, 7.6$ Hz, 1H), 7.24–7.38 (m, 3H), 7.39–7.65 (m, 3H), 8.27 (dd, $J = 1.6, 7.5$ Hz, 1H), 8.41 (ddd, $J = 1.5, 7.5, 19.3$ Hz, 2H), the H of tetrazole exchanges. MS m/z [M+H]⁺ Calcd for C₁₉H₁₈N₆O₂S: 394.1 Found: 395.1.

N-(4-(N-(3-(1H-tetrazol-5-yl)phenyl)sulfamoyl)phenyl)acetamide (4b). Pink solid (52% yield). ¹H NMR (400 MHz, DMSO-d₆) δ 2.12 (s, 3H), 7.31 (ddd, $J = 1.0, 2.3, 8.2$ Hz, 1H), 7.44 (t, $J = 7.9$ Hz, 1H), 7.65–7.72 (m, 3H), 7.74–7.79 (m, 2H), 7.86 (t, $J = 1.9$ Hz, 1H), the H of tetrazole exchanges. ¹³C NMR (100 MHz, DMSO-d₆) δ 22.58, 118.86, 118.95, 122.60, 123.07, 126.32, 127.96, 128.87, 129.96, 133.69, 139.01, 142.97, 170.57. MS m/z [M+H]⁺ Calcd for C₁₅H₁₄N₆O₃S: 358.1 Found: 359.2.

N-(3-(1H-tetrazol-5-yl)phenyl)quinoline-8-sulfonamide (5b). White solid (88% yield). ¹H NMR (400 MHz, Acetone-d₆) δ 7.28–7.42 (m, 2H), 7.59–7.90 (m, 4H), 8.03 (dt, $J = 1.1, 1.8$ Hz, 1H), 8.25 (dd, $J = 1.5, 8.2$ Hz, 1H), 8.42 (dd, $J = 1.4, 7.3$ Hz, 1H), 8.52 (dd, $J = 1.8, 8.4$ Hz, 1H), 9.21 (dd, $J = 1.8, 4.3$ Hz, 1H), 9.41 (s, 1H), the H of tetrazole exchanges. ¹³C NMR (100 MHz, Acetone-d₆) δ 117.35, 120.09, 123.01, 123.04, 125.55, 128.06, 129.17, 129.69, 129.79, 130.11, 133.27, 139.81, 140.02, 140.84, 149.72, 154.28. MS m/z [M+H]⁺ Calcd for C₁₆H₁₂N₆O₂S: 352.1 Found: 353.2.

N-(3-(1H-tetrazol-5-yl)phenyl)-4-chlorobenzenesulfonamide (6b). Light yellow solid (93% yield). ¹H NMR (400 MHz, Methanol-d₄) δ 7.57 (t, $J = 8.0$ Hz, 1H), 7.74 (dt, $J = 1.3, 7.9$ Hz, 2H), 7.78–7.84 (m, 1H), 7.99 (d, $J = 8.6$ Hz, 2H), 8.06 (d, $J = 8.6$ Hz, 2H), 8.41 (t, $J = 1.9$ Hz, 1H), the H of tetrazole exchanges. ¹³C NMR (100 MHz, Methanol-d₄) δ 117.35, 120.09, 123.01, 123.04, 125.55, 128.06, 129.17, 129.69, 129.79, 130.11, 133.27, 139.81, 140.02, 140.84, 149.72, 154.28. MS m/z [M+H]⁺ Calcd for C₁₃H₁₀ClN₅O₂S: 335.0, 337.0 Found: 336.1, 338.2.

Results and discussion

Virtual screening

The binding sites in the available KPC-2 crystal structures were analyzed to select a suitable receptor for docking. Alignment and superposition of the binding site residues of the seven available crystal structures of *E. coli* and *K. pneumoniae* KpKPC-2 revealed a rather rigid binding site with only Trp105 adopting two different rotamers, a closed conformation found 6-times and an open one, found two-times. In one structure, both rotamers were present (Fig 6). Thus, for virtual screening, the structure with the highest resolution was selected (*K. pneumoniae* KPC-2 in complex with the covalent inhibitor penamsulfone PSR-3-226 (PDB code

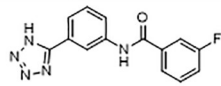
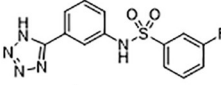
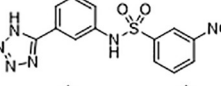
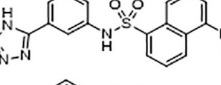
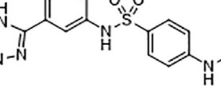
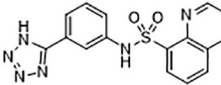
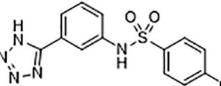
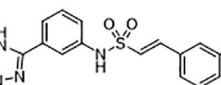
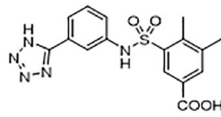
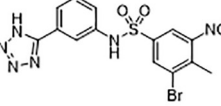
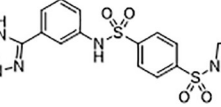
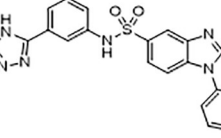
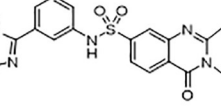
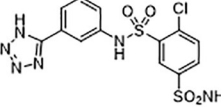
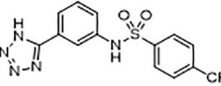
ID	STRUCTURE	IC ₅₀ mM ^[a,b]
11a		0.036
1b		> 0.2 (25)
2b		>0.6 (23)
3b		Not tested not soluble
4b		> 0.2 (16)
5b		> 0.2 (13)
6b		NI at 0.2
7b		>1.0 (30)
8b		> 1.0 (37)
9b		NI at 0.5
10b		NI at 0.5
11b		> 1.0 (37)
12b		NI at 0.5
13b		NI at 0.5
14b		>500 (20)

Fig 5. Inhibitory activity of 11a sulphonamide derivatives. ^[a] Assays were performed in duplicate (errors were less than 5%) with nitrocefin (114.28 μ M, K_m 36 μ M) as reporter substrate. Kinetic were monitored at 25° by following the absorbance variation at $\lambda = 485$ nm. ^[b] If no IC_{50} has been measured, percent inhibition at the highest tested concentration is given in parentheses. For example, > 1.0 (37%) implies that the highest concentration tested was 1.0 mM; at this concentration, the enzyme was inhibited by 37% and $IC_{50} > 1.0$ mM. When % Inhibition was below 10% No Inhibition (NI) is reported.

<https://doi.org/10.1371/journal.pone.0203241.g005>

3RXW), 1.26 Å resolution). This structure contained both rotamers of Trp105. For virtual screening, the closed conformation was chosen, as this is the most dominant conformation upon ligand binding.

Only little diversity with respect to bound ligands was found in the *KpKPC-2* structures. To obtain a more detailed picture on key interactions and to derive a pharmacophore hypothesis, PoSSuM—Search K was used to search for similar binding sites containing non-covalent ligands. This resulted in thirteen structures (Table 1), all having tetrazoles or carboxylates derivatives bound in the hydrophilic pocket formed by the amino acids corresponding to Thr235, Thr237, Ser130 and Ser70 in *KpKPC-2* (Fig 6). Seven of the contained ligands were fragment hits for *E.coli* CTX-M class A extended spectrum β -lactamase (ESBL), and four were derivatives of the most potent screening hit. Further, a structure of *S. fonticola* SFC-1 S70A β -lactamase in a non-covalent complex with meropenem and one of *E.coli* Toho-1 R274N: R276N β -lactamase in complex with a boronic acid were retrieved. Superposition of the binding site residues of *KpKPC-2* (PDB code 3RXW) and the CTX-M β -lactamase structures gave rmsd values for the $C\alpha$ atoms between 0.72 and 0.82 Å, for superposition of *KpKPC-2* and *S. fonticola* SFC-1 (PDB code 4EUZ) 0.28 Å and for superposition *KpKPC-2* and *E.coli* Toho-1 (PDB code 4BD0) 0.73 Å (Fig 7).

Based on the retrieved structures, a pharmacophore hypothesis was derived. All of the ligands in these structures as well as the β -lactamase binding protein (PDB code 3E2L, 3E2K) and the covalent ligand of the structure used as receptor, formed a hydrogen-bond with Thr235 or Thr237. Accordingly, a hydrogen-bond acceptor at the corresponding ligand position was considered to be crucial for binding (Fig 3). Further, in most of the structures the ligands formed interactions with Trp105 (Ambler numbering) [21]. Therefore, this interaction was also included in the pharmacophore hypothesis. Hydrogen-bond interactions to Asn130 were found in four structures (PDB codes 3RXW, 3G32, 3G30, 4EUZ) and included as well.

A hierarchical approach was adopted for virtual screening. First, our in-house database of around five million purchasable compounds was filtered for lead-like molecules [22]. In the second step, the obtained hits were screened with the above-described pharmacophore resulting in 44658 compounds. Out of these, 31122 compounds could be docked into the *KpKPC-2* binding site. Filtering these binding poses again with the pharmacophore resulted in 2894 compounds. These were divided into three clusters, depending on the functional group placed in the hydrophilic pocket (tetrazoles, carboxylates, sulfonamides) and inspected by eye. Finally, 32 compounds were selected for hit validation (Fig 4).

Most of the selected chemotypes carried an anionic group, mainly a carboxylic group or its bioisostere, the tetrazole ring. Candidates were predicted to orient the anionic side of their moiety in the carboxylic acid binding site of KPC-2, delimited by Ser130, Thr235 and Thr237 and present in all serine-based β -lactamases. In the above mentioned site, in fact, binds the C (3)4' carboxylate of β -lactams antibiotics as well as the sulfate group of avibactam and the carboxylic group of other known BLs inhibitors [12,31,36–38].

Hit evaluation

The large majority of the selected candidates were fragment-like as defined by the “rule of three” [39]. Dealing with fragments, potencies in the high micromolar to millimolar range

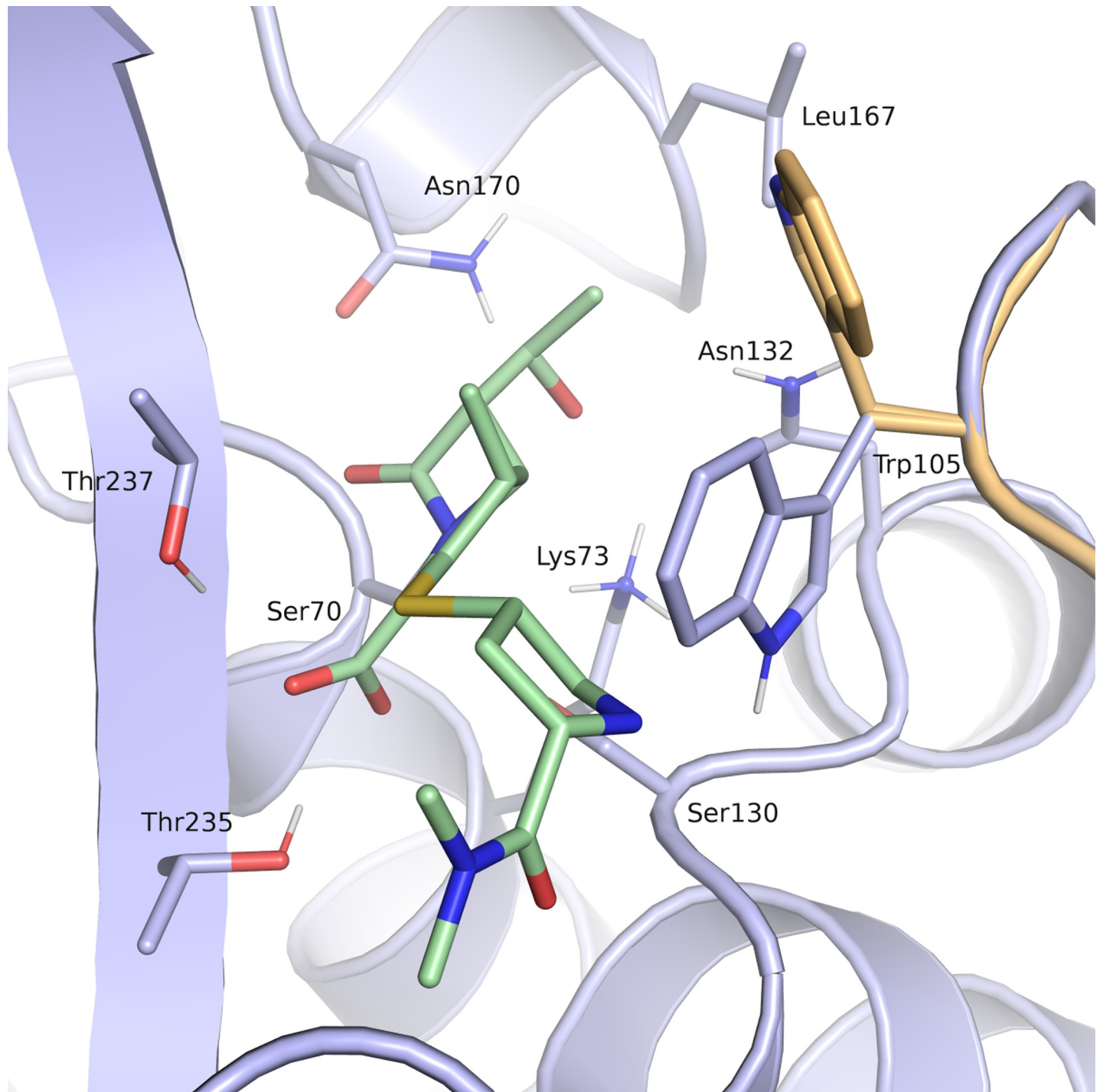


Fig 6. Binding site of *KpKPC-2* (PDB code 3RXW) with ligand meropenem (green, PDB code 4EUZ). The receptor conformation used for docking is coloured in blue, the rotamer of Trp105 not considered in the docking setup in beige (Ambler numbering) [21].

<https://doi.org/10.1371/journal.pone.0203241.g006>

were thus expected as well as others important issues such as reaching the solubility limit when testing the compounds and unpredictable precipitation in the employed assays conditions [40,41]. In our hands, the required high concentrations for ligand testing could not always be

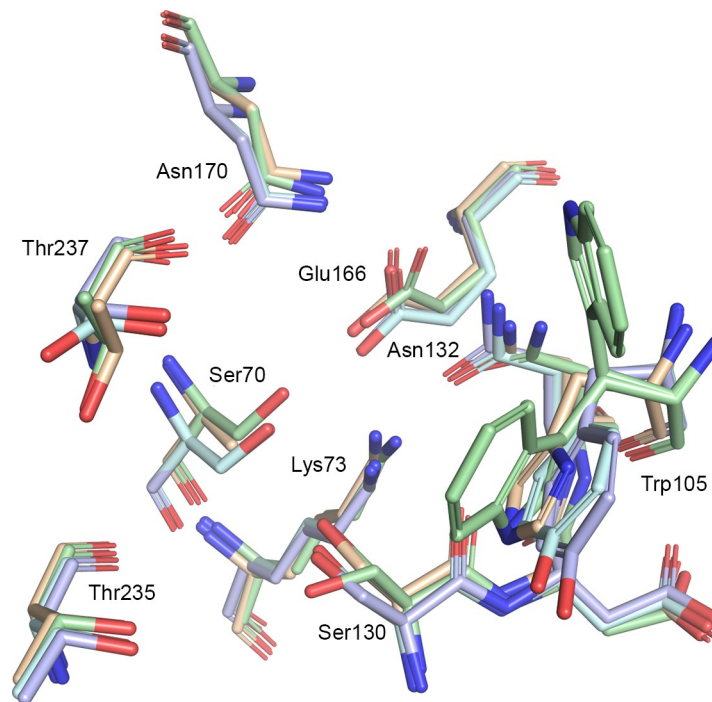


Fig 7. Analysis of PoSSuM hits. Superposition of the *Kp*KPC-2 binding site residues (PDB code 3RXW, green) with the *E. coli* CTX-M-9 β -lactamase (PDB code 4DDS, blue), the *S. fonticola* SFC-1 β -lactamase (PDB code 4EUZ, beige) and the *E. coli* TOHO-1 β -lactamase (PDB code 4BD0, cyan) (Ambler numbering) [21].

<https://doi.org/10.1371/journal.pone.0203241.g007>

achieved due to solubility which might have resulted in false negatives, but their true incidence is difficult to establish [42].

However, some of the tested molecules inhibited the hydrolytic activity of KPC-2 with low millimolar potency and their favorable solubility allowed us to determine full IC_{50} and/or K_i values. Among those, compounds **9a** and **11a** were the most promising compounds with micromolar affinities (IC_{50} of 0.15 and 0.036 mM, translating to ligand efficiencies (LE) of 0.38 and 0.28 kcal/mol/non-hydrogen atom, respectively; Fig 4) and were thus further investigated.

Compound **9a** was predicted to place its carboxylate group in proximity of the catalytic Ser70, in the carboxylic acid binding site mentioned above, forming hydrogen bond interactions with the side chains corresponding to amino acids Ser130, Thr235 and Thr237 (Fig 8). Thr 237 in KPC-2 is known to be necessary for cephalosporinase and carbapenemase activity and is involved in clavulanic acid, sulbactam and tazobactam recognition.[7] This position in β -lactamases that do not have carbapenemase or extended-spectrum β -lactamase (ESBL) activity generally corresponds to an alanine. The side chain hydroxyl groups of Ser130 and Ser70 were predicted to form interactions with the nitrogen of the benzothiazole ring. The predicted position of the aromatic system is well placed to establish ring-ring interactions with Trp105, a residue involved, in turn, in the stabilization of β -lactams through mainly hydrophobic and van der Waals interactions (centroids distances of 4.4 and 4.5 Å between Trp105 and the thiophene and the benzene rings respectively) The role of Trp105 in substrate and inhibitor interactions in KPC-2 β -lactamase has been deeply investigated being essential for hydrolysis of substrates.[7] The methoxy group of the molecule is oriented towards a rather open and solvent accessible area of the binding site and does not contact any of the surrounding residues. Interestingly, the presence of the sulphur atom of the benzothiazole system seems critical for

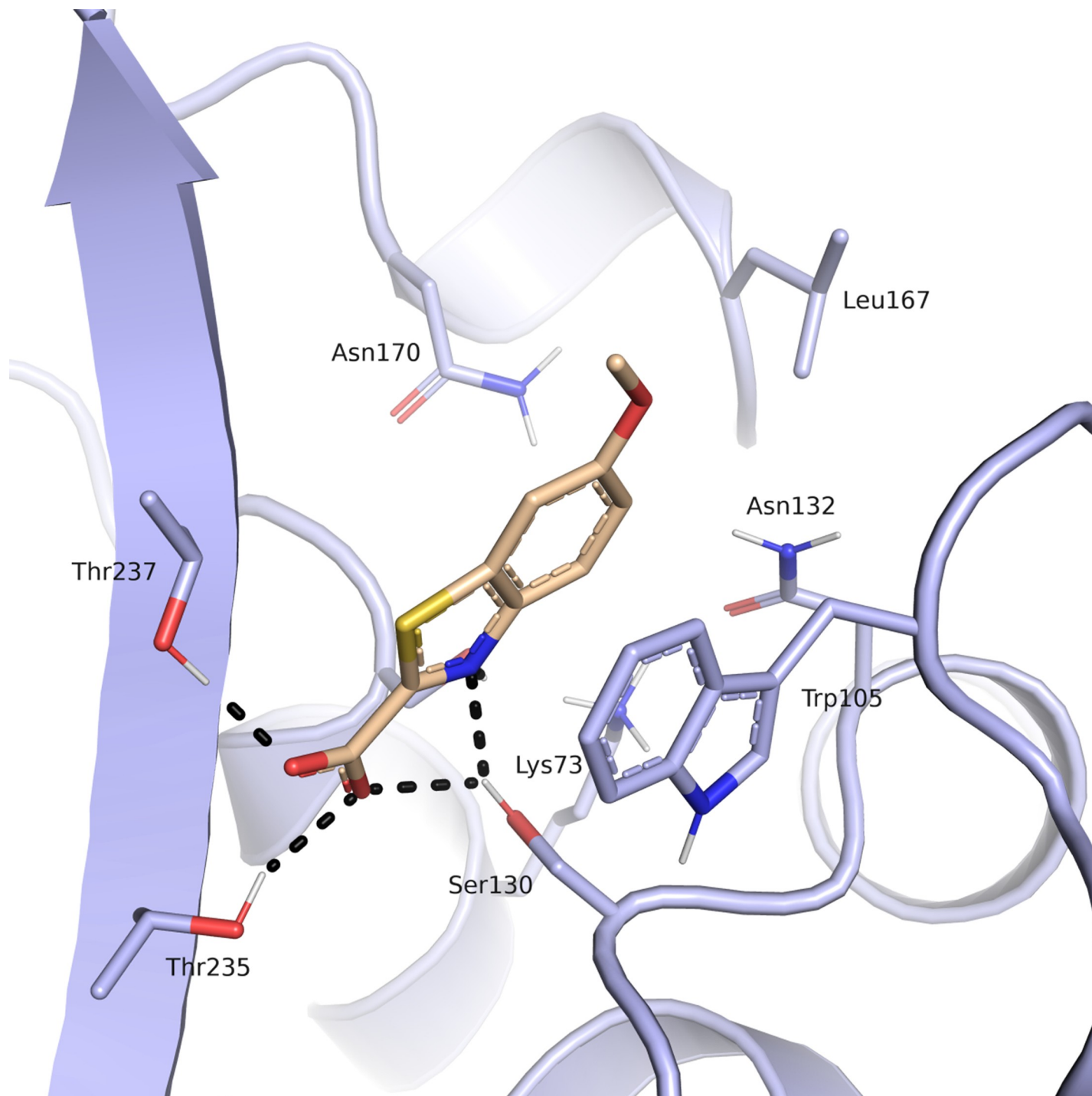


Fig 8. Predicted binding mode of compound 9a (beige) in the *KpKPC-2* receptor (blue). Putative hydrogen bond interactions are indicated as black dots (Ambler numbering)[21].

<https://doi.org/10.1371/journal.pone.0203241.g008>

affinity as the related compound **19a**, the benzimidazole analog, resulted 6-fold less active. Similar, the presence of the carboxylic group appeared to be crucial as compound **32a**, without such a functionality, was 8-fold less active.

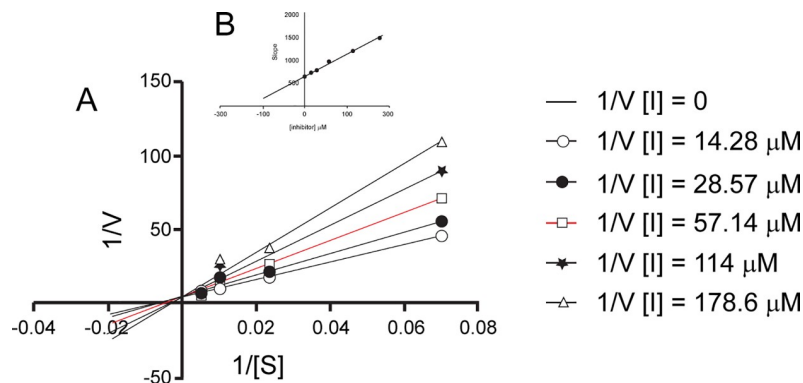


Fig 9. Determination of binding affinity and mode of inhibition of compound 9a. (A) Lineweaver-Burk plot (A) and Dixon slope plot (B).

<https://doi.org/10.1371/journal.pone.0203241.g009>

For compound **9a** binding affinity and mode of inhibition was determined by using gradient concentrations of CENTA. Fitting of the obtained data showed that compound **9a** behaves as a competitive inhibitor with a determined K_i of 112.0 μM (Fig 9). Its binding affinity was also determined towards other class A β -lactamases (IC_{50} vs CTX-M9 160 μM). For this compound aggregating behavior was also excluded by dynamic light scattering experiment (data not shown) [43]. Compound **9a** with its fragment-like characteristic (MW 208.21, determined K_i 112.0 μM , LE 0.38 kcal/mol/non-hydrogen atom) exerts an interesting activity vs KPC-2 and represents a very promising molecule to be directed to hit to lead optimization.

Among the 32 selected hits evaluated *in vitro* for their binding affinity vs KPC-2, compound **11a** was the most active inhibitor with a micromolar affinity vs KPC-2 (determined IC_{50} 36 μM , calculated K_i 14.8 μM , LE 0.28 kcal/mol/non-hydrogen atom). [35] The tetrazole ring of compound **11a**, a well-known bioisostere of the carboxylic group, was predicted to lie in the hydrophilic pocket formed by Thr235, Thr237, Ser130 and Ser70, driving the binding of the inhibitor in KPC-2 active site (Fig 10). The phenyl ring attached to the tetrazole was predicted to be sandwiched between the Trp105 side with a distance compatible with weak hydrophobic interactions and the backbone of Thr237. The amide group of **11a** was oriented in the canonical site delimited by Asn132, Asn170 and in a further distance Glu166 where the R1 amide side chain of β -lactams is known to bind. However, the amine linker and the second phenyl ring in **11a** were not predicted to form any specific interactions with the protein, except for the amide nitrogen contacting the backbone of Thr237. The distal fluoro-benzene ring was oriented at the entrance of the active site against two hydrophobic patches, one defined by Leu167, closer, and the other by the backbone of Asn170, a residue critical for carbapenemase activity.

Hit derivatization and evaluation

Compound **11a** appeared to be the most promising compound for optimization. Despite its small size, it has a potency in the low micromolar range (calculated K_i 14.8 μM) and a suitable ligand efficiency (0.28 kcal/mol/non-hydrogen atom). Therefore, this compound was selected to undergo chemical optimization for potency improvement and to investigate target binding requirements for optimal inhibitor-enzyme interaction. The phenyl-tetrazole moiety, that was predicted to strongly drive the binding, was retained unaltered, whereas structural modifications on the linker and on the distal aromatic ring were introduced in order to explore and maximize the interactions with the pocket formed by Asn132, Asn170 and Leu167 (Fig 10).

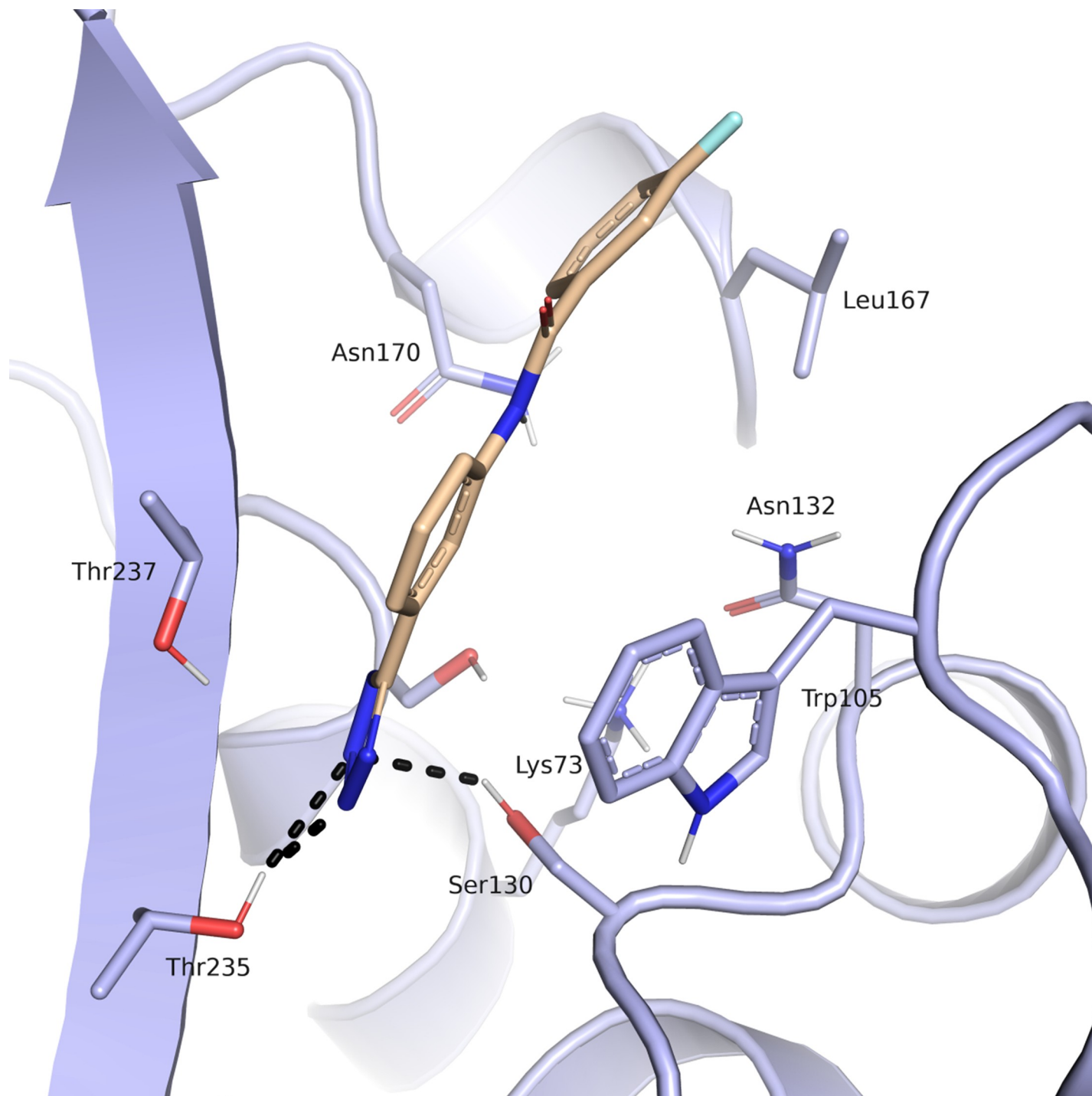


Fig 10. Predicted binding mode of compound 11a (beige) in the KpKPC-2 receptor (blue). Putative hydrogen bond interactions are indicated as black dots (Ambler numbering)[21].

<https://doi.org/10.1371/journal.pone.0203241.g010>

Because the amide linker does not contact efficaciously the protein we chose to replace it with a sulfonamide (Fig 11). We meant to target residues proximal to the opening of the active site while investigating the potentiality for sulfonamide derivatives.

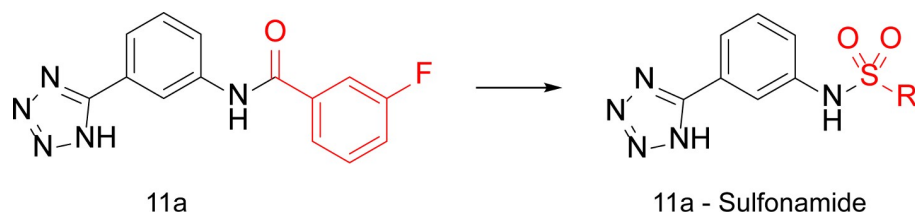


Fig 11. Design strategy for amide derivatives. Virtual Screening hit **11a** (left), amine **1** (black) and the optimized part of the molecule (red).

<https://doi.org/10.1371/journal.pone.0203241.g011>

Sulfonamides are more stable towards hydrolysis than carboxyamides, possess an additional hydrogen bonding oxygen atom and their NH is a strong hydrogen bond donor. In addition, the dihedral angle ω' OSNH measures around 90° compared with the 180° ω' OCNH angle of amide. Sulfonamides, in addition, have a non-planar configuration that could orient the distal ring towards Leu167 and Asn170 (Fig 12). Therefore, the introduction of a sp^3 geometry could allow a more efficacious spanning of the active site compared to the planar amide [44]. Moreover, modeling suggested that the sulfonamide group could form an additional hydrogen bond with Asn132 residue actively involved in substrate recognition and hydrolysis.

Further, we explored different substitutions on the sulfonamide linker to probe binding interactions. Substituents with different electronic and steric properties (i.e. halogens, nitro, sulfonamide, carboxylic acid, methyl, acetamide, amino groups) were inserted in the different position of the aromatic ring. In addition, the benzene ring was replaced by heterocyclic or extended benzofused systems such as benzimidazole, quinazolinone, naphthalene, or quinoxaline ring. Based on the availability of compound or building blocks, 6 compounds (**1b-6b**) were synthesized and 8 compounds (**7b-14b**) were purchased to test our hypothesis (Fig 5). The fourteen new compounds were tested *in vivo* vs clinical strains overproducing KPC-2 to evaluate their ability to restore bacteria susceptibility to carbapenem meropenem (Table 2).

Compounds **1b-6b** were synthesized in high yield (75–95% yield) and purity (>95%) through direct reaction of 3-(1H-tetrazol-5-yl) aniline and the appropriate sulfonyl chloride in dichloromethane at room temperature for 3 hours (Fig 13).

The derivatives of compound **11a** were tested for KPC-2 affinity (Fig 5). However, their solubility limit in the assay condition was often a limitation in accurate affinity determination. Overall, the compounds exhibited either weaker activities than **11a** or were not active at all at tested concentration. This data lets us confidentially affirm that the sulfonamide linker is not a suitable group to optimize the affinity of this compound series.

The antimicrobial activity of the best hits **9a** and **11a** and their derivatives was studied in bacterial cell cultures to investigate their ability to cross the outer membrane reaching the periplasmic space, where KPC-2 is secreted and confined in Gram negative bacteria. Compounds were tested for synergy with the β -lactam antibiotic meropenem against four *K. pneumoniae* clinical strains, isolated from different patients at the Hospital Universitario Son Espases, Palma de Mallorca, Spain. One of the four clinical strains was not a KPC-2 producer and was susceptible to meropenem (strain **Kpn (C-)**; MIC <0.25 μ g/mL). The three additional strains harbored the blaKPC-2 gene and were resistant to meropenem (Table 2). [32] Noteworthy none of the tested compounds had intrinsic antibiotic activity (MIC >256 μ g/mL), against the employed strains, included the susceptible one. The results show that in most cases the compounds were not able to reverse antibiotic resistance and did not showed synergism with meropenem. However, against strain Kpn 53A8 the MIC value was lowered by a factor of two when meropenem was combined with compounds **32a**, **1b**, **2b**, **5b** and **6b** while in combination with compound **11a** the MIC value was reduced by 4 fold.

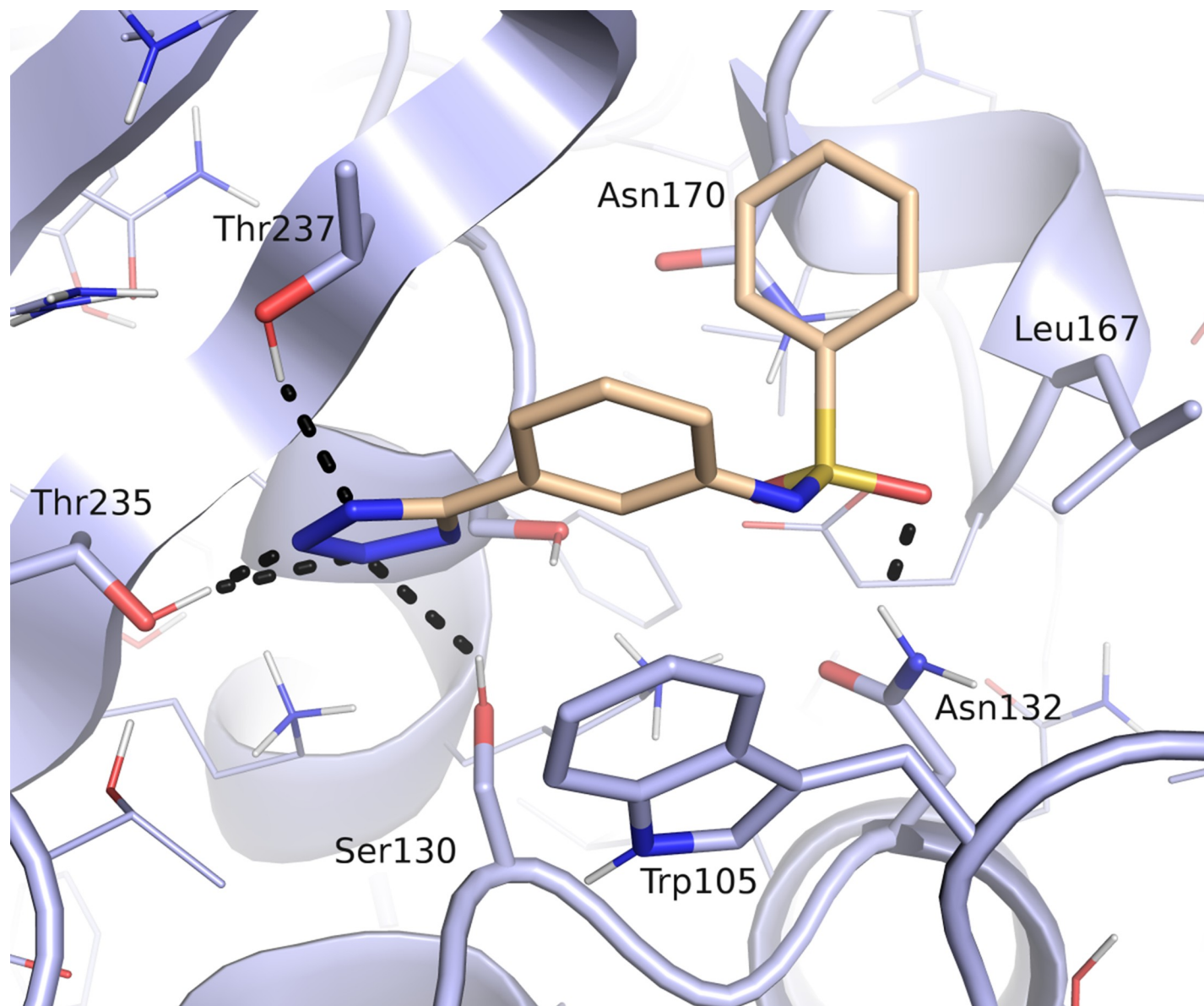


Fig 12. Predicted binding mode of a sulfonamide derivative of compound 11a (beige) in the *KpKPC-2* receptor (blue). Putative hydrogen bond interactions are indicated as black dots (Ambler numbering)[21].

<https://doi.org/10.1371/journal.pone.0203241.g012>

Conclusions

In this study two novel hits for KPC-2 were identified via an *in-silico* approach (compound 9 and 11a, Fig 4). Both of them had promising LEs with 0.38 and 0.28 kcal/mol/non-hydrogen atom, resp. 14 tetrazole derivatives originating from 11a were designed, synthesized and evaluated for their ability to inhibit KPC-2. We introduced chemical diversity on the distal part of the inhibitor, choosing to keep unchanged the anchor tetrazole ring while modifying the amide and the distal ring. The results suggest that a sulfonamide linker is neither suitable to improve the potency of 11a nor the solubility of final compounds. Future optimization work should instead rather concentrate on exploring secondary binding sites more distal from the pocket that the screening hits are supposed to address [45]. If the amide functionally found in

Table 2. *In vitro* interaction between meropenem and synthesized compounds vs *K. pneumoniae* clinical strains.

Code	MIC ^[a] meropenem in combination with synthesized compounds (1:1 molar) ^[a, b, c] ($\mu\text{g/mL}$)			
	Kpn (C-)	Kpn 99D8	Kpn 53A8	Kpn 53A9
—	<0.25	256	256	256
9a	<0.25	256	256	256
11a	<0.25	256	64	256
32a	<0.25	256	128	256
1b	<0.25	256	128	256
2b	<0.25	256	128	256
4b	<0.25	256	256	256
5b	<0.25	256	128	256
6b	<0.25	256	128	256

^[a] Assays were conducted against four *K. pneumoniae* clinical strains isolated from different patients at the Hospital Universitario Son Espases, Palma de Mallorca, Spain. MICs were determined according to EUCAST standards and the presented values are the median of three independent experiments.

^[b] Compounds were tested alone and showed no activity (MIC > 256) in all cases.

^[c] Strain C- is control *K. pneumoniae* and meropenem susceptible (MIC < 0.25 $\mu\text{g/mL}$)

<https://doi.org/10.1371/journal.pone.0203241.t002>

11a or alternative linkers are best suited remains to be explored. Nevertheless, two promising hit compounds for KPC-2 were retrieved which can serve as starting points to derive more potent inhibitors.

Although a decrease of potency in *in vitro* tests was registered for the designed and synthesized chemical entities, as none of the compounds was able to trigger stronger interactions with the open region of KPC-2 they were meant to target, this study yielded a better comprehension of the catalytic pocket of this enzyme. Our study provided a better understanding of how challenging the target of additional, superficial, binding pockets is and how it could be critical in designing inhibitors with improved potency, especially in area proximal to the active site opening.

The (1H-tetrazol-5-yl)phenyl ring was most frequent among the high scoring candidates in our *in silico* study, suggesting that this functionality is well suited to anchor ligands in the KPC-2 binding site. The rather weak affinity of the ligands hints that rest of the ligand, i.e. the

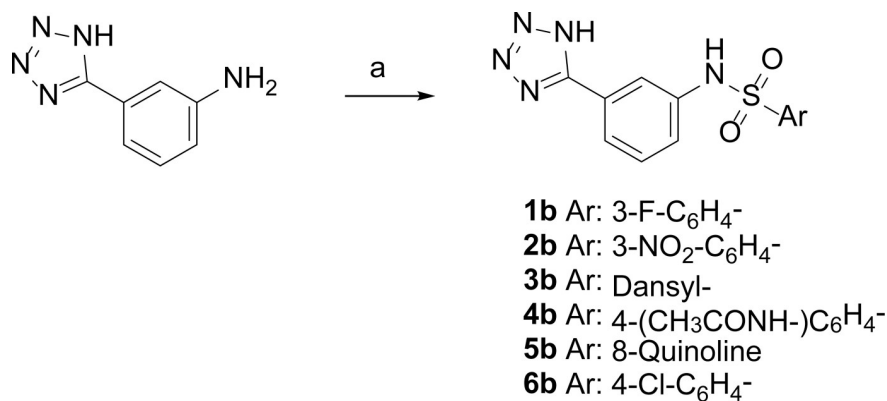


Fig 13. Reagents and conditions. a) aryl-sulfonyl chloride (1.2 eq.), pyridine (3 eq.), dry DCM, N₂, r.t, 3 h, 75–95% yield.

<https://doi.org/10.1371/journal.pone.0203241.g013>

functional groups out of the center phenyl ring and the amide linker, need to be optimized to increase potency. However, introducing a sulfonamide linker was detrimental for potency. We hypothesize that the presence of a sulfonamide instead of an amide led to a rearrangement of the ligand in the binding site to minimize steric hindrance, and thus resulted in the loss of key interactions. These rearrangements can be particularly critical in non-covalent inhibitors like ours that are not stabilized by a covalent interaction with the catalytic serine, as this type of inhibitors are supposed to have lower residence times with respect to covalent β -lactamase inhibitors (Fig 1). In designing larger and more potent inhibitors, additional secondary binding sites which have been found to be critical for affinity improvement need to be considered [45].

The difficulties in optimizing the affinity of hit **11a** for its target are also caused by the lack of an accurate 3D structure of the complex. While reliable methods using docking can be obtained, experimental confirmation of the binding modes is desirable to make sure that no wrong tracks are followed [46]. In the case of compound **11a**, we are more certain about the position of the tetrazole moiety in the binding site due to the availability of crystal structures of related targets with similar ligands (Table 1) while the placement of the substituent we attempted to optimize is more tentative. Further structural work and medicinal chemistry work is ongoing to significantly increase the potency of the most promising compound **11a** *in vitro* and *in vivo* and new chemistry is under evaluation for these derivatives, taking advantage of other additional recognition sites in KPC-2.

Acknowledgments

We thank Hayarpi Torosyan from Brian K Shoichet's Laboratory at USCF for dynamic light scattering measurements on compound **9a**, Josef Kehrein for contributions to the modelling work, and Openeye for free software licenses. Virtual screening was performed on resources provided by UNINETT Sigma2—the National Infrastructure for High Performance Computing and Data Storage in Norway and the Mogon cluster of the Johannes Gutenberg University Mainz.

Author Contributions

Conceptualization: Raphael Klein, Ruth Brenk, Donatella Tondi.

Formal analysis: Pasquale Linciano.

Funding acquisition: Donatella Tondi.

Investigation: Raphael Klein, Pasquale Linciano, Pierangelo Bellio, Sofia Papaioannou, Jesus Blazquez, Donatella Tondi.

Methodology: Pasquale Linciano, Pierangelo Bellio.

Project administration: Donatella Tondi.

Resources: Giuseppe Celenza, Laura Cendron.

Supervision: Ruth Brenk, Donatella Tondi.

Visualization: Raphael Klein, Pasquale Linciano.

Writing – original draft: Raphael Klein, Pasquale Linciano, Ruth Brenk, Donatella Tondi.

References

1. Papp-Wallace KM, Endimiani A, Taracila MA, Bonomo RA. Carbapenems: Past, present, and future. *Antimicrob Agents Chemother*. 2011; 55: 4943–4960. <https://doi.org/10.1128/AAC.00296-11> PMID: 21859938
2. Tondi D, Cross S, Venturelli A, Costi MP, Cruciani G, Spyrakis F. Decoding the Structural Basis For Carbapenem Hydrolysis By Class A β -lactamases: Fishing For A Pharmacophore. *Curr Drug Targets*. Netherlands; 2016; 17: 983–1005. PMID: 26424401
3. Livermore DM, Woodford N. The β -lactamase threat in Enterobacteriaceae, Pseudomonas and Acinetobacter. *Trends Microbiol*. England; 2006; 14: 413–420. <https://doi.org/10.1016/j.tim.2006.07.008> PMID: 16876996
4. Farina D, Spyrakis F, Venturelli A, Cross S, Tondi D, Paola Costi M. The Inhibition of Extended Spectrum β -Lactamases: Hits and Leads. *Current Medicinal Chemistry*. 2014, pp. 1405–1434. PMID: 24180276
5. Frère J-M, Sauvage E, Kerff F. From “An Enzyme Able to Destroy Penicillin” to Carbapenemases: 70 Years of β -lactamase Misbehaviour. *Current Drug Targets*. 2016, pp. 974–982. PMID: 26424390
6. Naas T, Dortet L, Iorga B. Structural and Functional Aspects of Class A Carbapenemases. *Current Drug Targets*. 2016, pp. 1006–1028. <https://doi.org/10.2174/1389450117666160310144501> PMID: 26960341
7. Papp-Wallace KM, Bethel CR, Distler AM, Kasuboski C, Taracila M, Bonomo RA. Inhibitor resistance in the KPC-2 β -lactamase, a preeminent property of this class A β -lactamase. *Antimicrob Agents Chemother*. United States; 2010; 54: 890–897. <https://doi.org/10.1128/AAC.00693-09> PMID: 20008772
8. Brem J, Cain R, Cahill S, McDonough MA, Clifton IJ, Jiménez-Castellanos J-C, et al. Structural basis of metallo- β -lactamase, serine- β -lactamase and penicillin-binding protein inhibition by cyclic boronates. 2016; 7: 12406. <https://doi.org/10.1038/ncomms12406> PMID: 27499424
9. Santucci M, Spyrakis F, Cross S, Quotadamo A, Farina D, Tondi D, et al. Computational and biological profile of boronic acids for the detection of bacterial serine- and metallo- β -lactamases. *Sci Rep*. 2017; 7: 1–15. <https://doi.org/10.1038/s41598-016-0028-x>
10. Danishuddin M, Khan AU. Structure based virtual screening to discover putative drug candidates: Necessary considerations and successful case studies. *Methods*. 2015; 71: 135–145. <https://doi.org/10.1016/j.jymeth.2014.10.019> PMID: 25448480
11. Khan A, Faheem M, Danishuddin M, Khan AU. Evaluation of Inhibitory Action of Novel Non β -Lactam Inhibitor against *Klebsiella pneumoniae* Carbapenemase (KPC-2). *PLoS One*. Public Library of Science; 2014; 9: e108246. <https://doi.org/10.1371/journal.pone.0108246> PMID: 25265157
12. Krishnan NP, Nguyen NQ, Papp-Wallace KM, Bonomo RA, van den Akker F. Inhibition of *Klebsiella* β -Lactamases (SHV-1 and KPC-2) by Avibactam: A Structural Study. *PLoS One*. Public Library of Science; 2015; 10: e0136813. <https://doi.org/10.1371/journal.pone.0136813> PMID: 26340563
13. Pemberton OA, Zhang X, Chen Y. Molecular Basis of Substrate Recognition and Product Release by the *Klebsiella pneumoniae* Carbapenemase (KPC-2). *J Med Chem*. United States; 2017; 60: 3525–3530. <https://doi.org/10.1021/acs.jmedchem.7b00158> PMID: 28388065
14. Ito JI, Tabei Y, Shimizu K, Tsuda K, Tomii K. PoSSuM: A database of similar protein-ligand binding and putative pockets. *Nucleic Acids Res*. 2012; 40: 541–548. <https://doi.org/10.1093/nar/gkr701>
15. Ito JI, Ikeda K, Yamada K, Mizuguchi K, Tomii K. PoSSuM v.2.0: Data update and a new function for investigating ligand analogs and target proteins of small-molecule drugs. *Nucleic Acids Res*. 2015; 43: D392–D398. <https://doi.org/10.1093/nar/gku1144> PMID: 25404129
16. Ke W, Bethel CR, Papp-Wallace KM, Pagadala SRR, Nottingham M, Fernandez D, et al. Crystal structures of KPC-2 β -lactamase in complex with 3-nitrophenyl boronic acid and the penam sulfone PSR-3-226. *Antimicrob Agents Chemother*. United States; 2012; 56: 2713–2718. <https://doi.org/10.1128/AAC.06099-11> PMID: 22330909
17. Nichols DA, Jaishankar P, Larson W, Smith E, Liu G, Beyrouthy R, et al. Structure-based design of potent and ligand-efficient inhibitors of CTX-M class A β -lactamase. *J Med Chem*. 2012; 55: 2163–2172. <https://doi.org/10.1021/jm2014138> PMID: 22296601
18. Tomanicek SJ, Standaert RF, Weiss KL, Ostermann A, Schrader TE, Ng JD, et al. Neutron and X-ray Crystal Structures of a Perdeuterated Enzyme Inhibitor Complex Reveal the Catalytic Proton Network of the Toho-1 β -Lactamase for the Acylation Reaction. *J Biol Chem*. 9650 Rockville Pike, Bethesda, MD 20814, U.S.A.: American Society for Biochemistry and Molecular Biology; 2013; 288: 4715–4722. <https://doi.org/10.1074/jbc.M112.436238> PMID: 23255594
19. Chen Y, Shoichet BK. Molecular docking and ligand specificity in fragment-based inhibitor discovery. *Nat Chem Biol*. 2009; 5: 358–364. <https://doi.org/10.1038/nchembio.155> PMID: 19305397

20. Fonseca F, Chudyk EI, van der Kamp MW, Correia A, Mulholland AJ, Spencer J. The Basis for Carbapenem Hydrolysis by Class A β -Lactamases: A Combined Investigation using Crystallography and Simulations. *J Am Chem Soc. American Chemical Society*; 2012; 134: 18275–18285. <https://doi.org/10.1021/ja3044460j> PMID: 23030300
21. Ambler RP, Coulson AF, Frere JM, Ghuysen JM, Joris B, Forsman M, et al. A standard numbering scheme for the class A beta-lactamases. *The Biochemical journal. England*; 1991. pp. 269–270.
22. Brenk R, Schipani A, James D, Krasowski A, Gilbert IH, Frearson J, et al. Lessons learnt from assembling screening libraries for drug discovery for neglected diseases. *ChemMedChem*. 2008; 3: 435–444. <https://doi.org/10.1002/cmdc.200700139> PMID: 18064617
23. Hawkins PCD, Skillman AG, Warren GL, Ellingson BA, Stahl MT. Conformer Generation with OMEGA: Algorithm and Validation Using High Quality Structures from the Protein Databank and Cambridge Structural Database. *J Chem Inf Model. American Chemical Society*; 2010; 50: 572–584. <https://doi.org/10.1021/ci100031x> PMID: 20235588
24. Mpamhanga CP, Spinks D, Tulloch LB, Shanks EJ, Robinson DA, Collie IT, et al. One scaffold, three binding modes: Novel and selective pteridine reductase 1 inhibitors derived from fragment hits discovered by virtual screening. *J Med Chem*. 2009; 52: 4454–4465. <https://doi.org/10.1021/jm900414x> PMID: 19527033
25. Brenk R, Irwin JJ, Shoichet BK. Here Be Dragons: Docking and Screening in an Uncharted Region of Chemical Space. *J Biomol Screen*. 2005; 10: 667–674. <https://doi.org/10.1177/1087057105281047> PMID: 16170052
26. Mysinger MM, Shoichet BK. Rapid context-dependent ligand desolvation in molecular docking. *J Chem Inf Model*. 2010; 50: 1561–1573. <https://doi.org/10.1021/ci100214a> PMID: 20735049
27. Lorber DM, Shoichet BK. Flexible ligand docking using conformational ensembles. *Protein Sci*. 1998; 7: 938–950. <https://doi.org/10.1002/pro.5560070411> PMID: 9568900
28. Wei BQ, Baase WA, Weaver LH, Matthews BW, Shoichet BK. A Model Binding Site for Testing Scoring Functions in Molecular Docking. *J Mol Biol*. 2002; 322: 339–355. [https://doi.org/10.1016/S0022-2836\(02\)00777-5](https://doi.org/10.1016/S0022-2836(02)00777-5) PMID: 12217695
29. Kuntz ID, Chen K, Sharp KA, Kollman PA. The maximal affinity of ligands. *Proc Natl Acad Sci*. 1999; 96: 9997–10002. PMID: 10468550
30. Hopkins AL, Groom CR, Alex A. Ligand efficiency: a useful metric for lead selection. *Drug Discov Today*. 2004; 9: 430–431. [https://doi.org/10.1016/S1359-6446\(04\)03069-7](https://doi.org/10.1016/S1359-6446(04)03069-7) PMID: 15109945
31. Celenza G, Vicario M, Bellio P, Linciano P, Perilli M, Oliver A, et al. Phenylboronic Acid Derivatives as Validated Leads Active in Clinical Strains Overexpressing KPC-2: A Step against Bacterial Resistance. *ChemMedChem*. 2018; <https://doi.org/10.1002/cmdc.201700788> PMID: 29356380
32. Crompton R, Williams H, Ansell D, Campbell L, Holden K, Cruickshank S, et al. Oestrogen promotes healing in a bacterial LPS model of delayed cutaneous wound repair. *Lab Invest. United States*; 2016; 96: 439–449. <https://doi.org/10.1038/labinvest.2015.160> PMID: 26855364
33. Feng BY, Shoichet BK. A detergent-based assay for the detection of promiscuous inhibitors. *Nat Protoc. England*; 2006; 1: 550–553. <https://doi.org/10.1038/nprot.2006.77> PMID: 17191086
34. Quotadamo A, Linciano P, Davoli P, Tondi D, Costi MP, Venturelli A. An Improved Synthesis of CENTA, a Chromogenic Substrate for β -Lactamases. *Synlett*. 2016; 27: 2447–2450. <https://doi.org/10.1055/s-0035-1562454>
35. Cheng Y, Prusoff WH. Relationship between the inhibition constant (K_1) and the concentration of inhibitor which causes 50 per cent inhibition (I_{50}) of an enzymatic reaction. *Biochem Pharmacol. England*; 1973; 22: 3099–3108. PMID: 4202581
36. Strynadka NC, Adachi H, Jensen SE, Johns K, Sielecki A, Betzel C, et al. Molecular structure of the acyl-enzyme intermediate in beta-lactam hydrolysis at 1.7 Å resolution. *Nature. England*; 1992; 359: 700–705. <https://doi.org/10.1038/359700a0> PMID: 1436034
37. Tondi D, Venturelli A, Bonnet R, Pozzi C, Shoichet BK, Costi MP. Targeting class A and C serine beta-lactamases with a broad-spectrum boronic acid derivative. *J Med Chem. United States*; 2014; 57: 5449–5458. <https://doi.org/10.1021/jm5006572> PMID: 24882105
38. Genovese F, Lazzari S, Venturi E, Costantino L, Blazquez J, Ibacache-Quiroga C, et al. Design, synthesis and biological evaluation of non-covalent AmpC β -lactamases inhibitors. *Med Chem Res*. 2017; 26: 975–986. <https://doi.org/10.1007/s00044-017-1809-x>
39. Congreve M, Carr R, Murray C, Jhoti H. A “rule of three” for fragment-based lead discovery? *Drug Discov Today. England*; 2003; 8: 876–877.
40. Popa-Burke I, Russell J. Compound precipitation in high-concentration DMSO solutions. *J Biomol Screen*. 2014; 19: 1302–1308. <https://doi.org/10.1177/1087057114541146> PMID: 24980595

41. Bembenek SD, Tounge BA, Reynolds CH. Ligand efficiency and fragment-based drug discovery. *Drug Discov Today*. 2009; 14: 278–283. <https://doi.org/10.1016/j.drudis.2008.11.007> PMID: 19073276
42. Popa-Burke IG, Issakova O, Arroway JD, Bernasconi P, Chen M, Coudurier L, et al. Streamlined system for purifying and quantifying a diverse library of compounds and the effect of compound concentration measurements on the accurate interpretation of biological assay results. *Anal Chem*. 2004; 76: 7278–7287. <https://doi.org/10.1021/ac0491859> PMID: 15595870
43. Seidler J, McGovern SL, Doman TN, Shoichet BK. Identification and Prediction of Promiscuous Aggregating Inhibitors among Known Drugs. *J Med Chem*. American Chemical Society; 2003; 46: 4477–4486. <https://doi.org/10.1021/jm030191r> PMID: 14521410
44. Vijayadas KN, Davis HC, Kotmale AS, Gawade RL, Puranik VG, Rajamohanam PR, et al. An unusual conformational similarity of two peptide folds featuring sulfonamide and carboxamide on the backbone. *Chem Commun*. The Royal Society of Chemistry; 2012; 48: 9747–9749. <https://doi.org/10.1039/C2CC34533A> PMID: 22914747
45. Babaoglu K, Shoichet BK. Deconstructing fragment-based inhibitor discovery. *Nature chemical biology*. United States; 2006. pp. 720–723. <https://doi.org/10.1038/nchembio831> PMID: 17072304
46. Verdonk ML, Giangreco I, Hall RJ, Korb O, Mortenson PN, Murray CW. Docking Performance of Fragments and Druglike Compounds. *J Med Chem*. American Chemical Society; 2011; 54: 5422–5431. <https://doi.org/10.1021/jm200558u> PMID: 21692478